Impacts of Land Surface on Climate of July and Onset of Summer Monsoon: A Study with an AGCM plus SSiB①

Liu Hui (刘 辉) and *Wu Guoxiong* (吴国雄)

State Key Laboratory of Numerical Modelling for Atmospheric Sciences and Geophysical Fluid Dynamics (LASG), Institute of Atmospheric Physics, Chinese Academy of Sciences, Beijing, 100080

Received October 27, 1996, revised December 24, 1996

ABSTRACT

To get more insight into the impacts of land surface processes on climate, a simplified biosphere model (SSiB) developed by Sellers and Xue et al. is implemented into the LASG / IAP spectral climate AGCM(R15L9). The new model has been integrated for more than twenty years. The diagnoses of the integration show that the implementing of the land surface processes has greatly improved the simulation of July climate. It is also shown that the seasonal variations of land surface characteristics have great impacts on the onset of summer monsoon, especially the seasonal march of wind at 850 hPa and precipitation over the regions of summer monsoon.

Key words: AGCM plus SSiB, Impacts of land surface processes

I. INTRODUCTION

We know that characteristics of land surface of our earth are quite different from one place to another. About 50 percent of the land surface is covered by vegetation and the types of vegetation vary greatly from one area to another. The remained parts are composed of bare soil and snow, about 25 percent each (Fig. 1). This will result in global differences in exchanges of heat and water between the land surface and atmosphere and so will have impacts on the global climate of atmosphere. In addition, the land surface, especially the vegetation, has great seasonal variations, especially over Asia. These seasonal variation will result in seasonal variations in roughness, albedo, and evapotranspiration from deep soil to atmosphere and so will have impacts on the heat and water exchanges between the atmosphere and the surface. To get more insight into these exchanges of heat and water between the atmosphere and the land surface as well as their impacts on climate, a few more sophistic numerical biospherical models have been developed in recent years. One of them is the biospherical model(SSiB) developed by Sellers and Xue (Sellers et al., 1986; Xue et al., 1991). Here the SSiB model is implemented into the LASG / IAP 9-layer spectral AGCM to study the impacts of the land surface processes on climate, especially the climate of East Asia. In the first part of the paper, the model is described briefly, then the impacts of the global differences in land surface characteristics on July mean climate of the AGCM will be presented. In the third part, the impacts of the seasonal variations of the land surface on the march of precipitation and 850 hPa wind during the onset of summer monsoon will be presented.

①This research is supported by the CNSF Key program "The mechanism of the variation of subtropical high" No. 49635170 and the CNSF projects No. 49575265, 49475255, and 49475259.

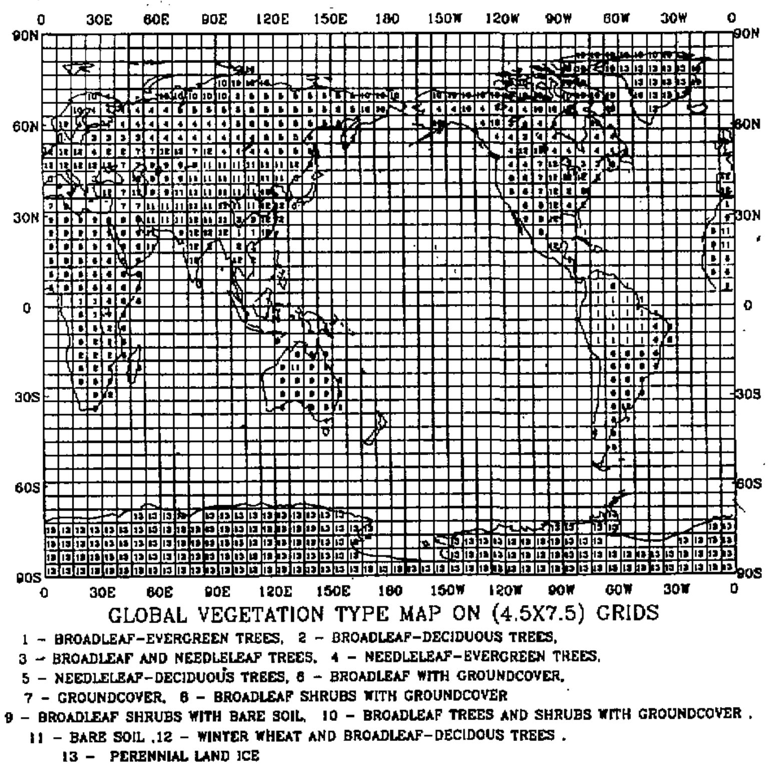

Fig. 1. Distribution of global vegetation type on Gaussian grid(R15).

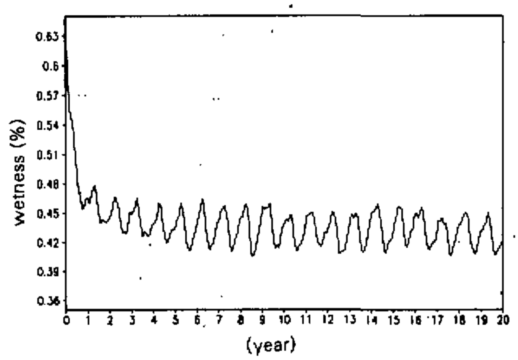

Fig. 2. Time evolution of global mean wetness of the first soil layer for the 20-year integration of the SSiB-AGCM.

II. THE MODEL

The original version of the AGCM (control AGCM) is a nine-layer spectral (R15) climate AGCM developed in LASG / IAP (Wu et al., 1996). In that version, the wetness of the

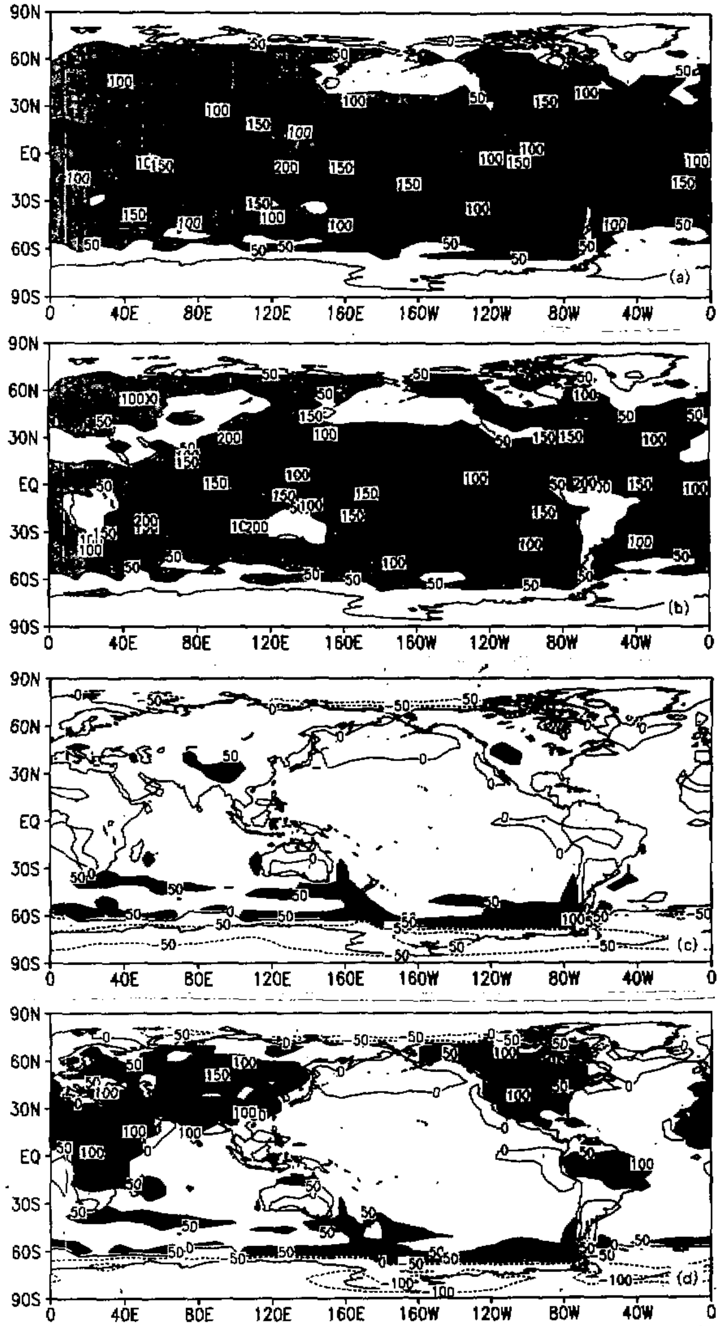

Fig. 3. The latent (a and b) and sensible heat flux(c and d) in July averaged for the last 15 years for the control AGCM run and SSiB–AGCM run, respectively. Unit: W / m^2.

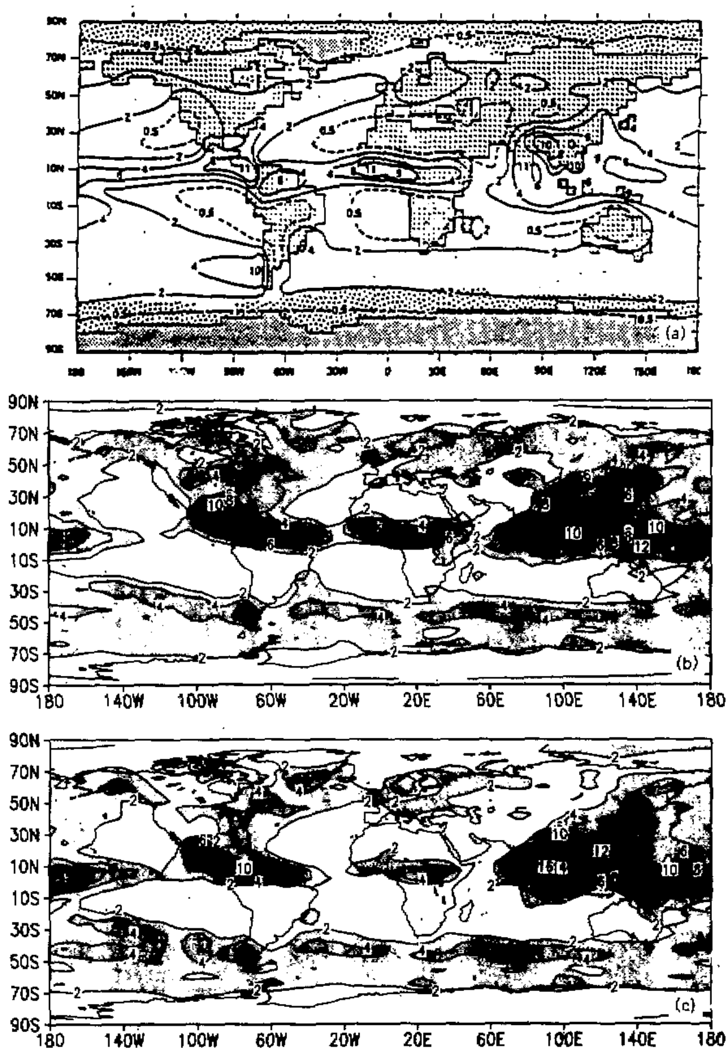

Fig. 4. Global distribution of precipitation in July. (a): observation from Schutz and Gates(1971,1972); (b): control AGCM run; (c): SSiB–AGCM run. Unit: mm / day.

land surface is assumed as constant of 0.25 and the roughness of 0.3 m. The snow cover over land is prescribed according to observation. The boundary exchanges between the surface and the atmosphere are given by the bulk aero–dynamic parameterization in which the same aerodynamical resistance is used to describe the heat and water exchanges. The diurnal variation of solar insolation is not considered in the model at the moment. The SST and sea ice forcing in the model are taken from AMIP dataset without interannual variability.

The SSiB model (Xue et al., 1991), which is a simplified version of the Simple Biosphere model(SiB) of Sellers et al.(1986), is used to simulate the land surface in the coupled model. In SSiB, there are one vegetation layer and three soil layers. It includes eight prognostic variables: soil wetness in the three soil layers; temperatures at the canopy, ground surface and in deep soil layer; water storage on the canopy; and snow stored on the ground.

There are eleven vegetation types in SSiB. These include tall vegetation, short vegetation, arable crops. In addition, one bare soil and one snow are included. A parameter set for each of the 11 vegetation types was obtained based on a variety of sources. Some parameters were derived from calibrations of field measurements. Many parameters were derived from the biometrics and physiological data for representative species in each biome determined from a wide–range survey of the ecological and geographical literature (Doman and Sellers, 1989; Willmott and Klink, 1986). Seasonally varying monthly values of leaf area index, roughness, and green leaf fraction are prescribed. Klink and Wilmott (1985) compiled charts of leaf area index and green leaf fraction annual cycles for each Kuchler vegetation type. The seasonal variations of the leaf area index and green leaf fraction are based on these charts. The prescription of the crop vegetation is different: the vegetation cover, leaf area index, green leaf fraction, leaf orientation, and root length are varied according to the growing season, which is a function of latitude and time.

The Force–restored method is used to predict the time variation of the soil temperatures. In the three layers of soil, water movement is described by a finite–difference approximation to the diffusion equations. The governing equations for the interception water stores are based on water conservation equations.

The implementing scheme is preliminary. The atmospheric forcings for SSiB, i.e., air temperature, water mixing ratio and wind, are taken directly from the lowest level of the AGCM, i.e., about 70 meters high. The nonlinear vertical diffusion of the original version of the AGCM is used to exchange the heat, water, and momentum between the lowest layer and upper layers of the AGCM. The boundary layer scheme of the origional AGCM is kept over non–land area, that is, over sea and sea ice areas. The SSiB is computed on each model time step, that is, 30 minutes.

The main difference of the land surface processes in the SSiB–AGCM from the surface parameterization used in the control AGCM is that there is one extra way to transfer water to atmosphere from deep soil through vegetation root system, even when the top soil layer is dry. This makes the water flow into atmosphere larger over tall vegetation which has dense root systems. In addition, the SSiB model will increase the ratio of sensible heat flux over latent heat flux than the control AGCM in most situation, which seems to be more reasonable (Sato et al., 1989). The wetness and snow amount predicted in SSiB will also introduce more feedbacks between the surface and the atmosphere than the control AGCM.

The control AGCM has been integrated for 50 model years before the implementing. In the SSiB–AGCM run, the atmospheric component starts from the equilibrium of Dec. 31 of year 50 of the control AGCM. The canopy and ground surface water storage are initialized everywhere to zero, and the ground and deep soil temperatures are set equal to ground surface temperature of Dec. 31 of the year 50. The soil moisture at the three model layers is initialized with a constant of 0.25 out of tropics and 0.85 within tropics, which is very artificial. From that state, both the SSiB–AGCM and control AGCM have been integrated for 20 years.

Fig. 2 shows the time–evolution of the global mean wetness of the first soil layer for that period. It is clear that the soil moisture has experienced an abrupt adjustment for the first year

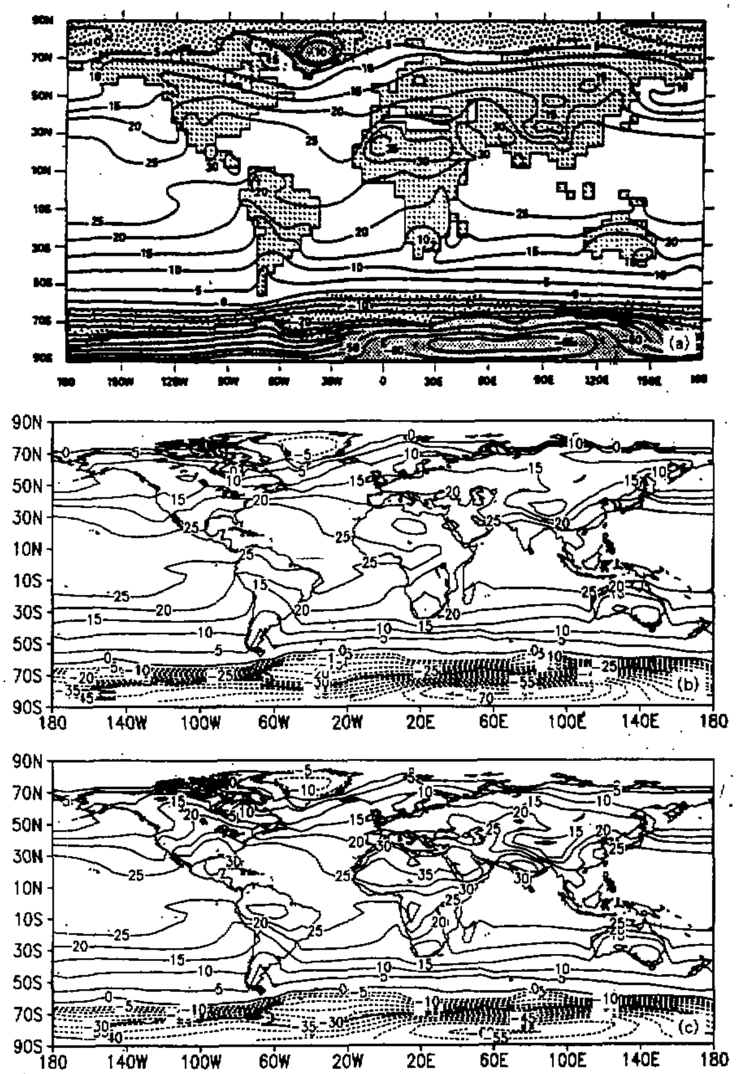

Fig. 5. Global distribution of surface temperature in July. (a): observation from Schlesinger and Gates(1980); (b): control AGCM run; (c): SSiB–AGCM run. Unit: hPa.

and a slower adjustment for the next few years from the artificial start state. It then fluctuates around an equilibrium from the 6th year onwards. The deep ground temperature has similar evolution characteristic. So, the SSiB–AGCM can be thought to reach an equilibrium since year 6 onward and the following analyses are all taken from the last 15 years.

III. CLIMATE OF JULY

From the global distribution of the vegetation types (shown in Fig. 1), it can be seen that

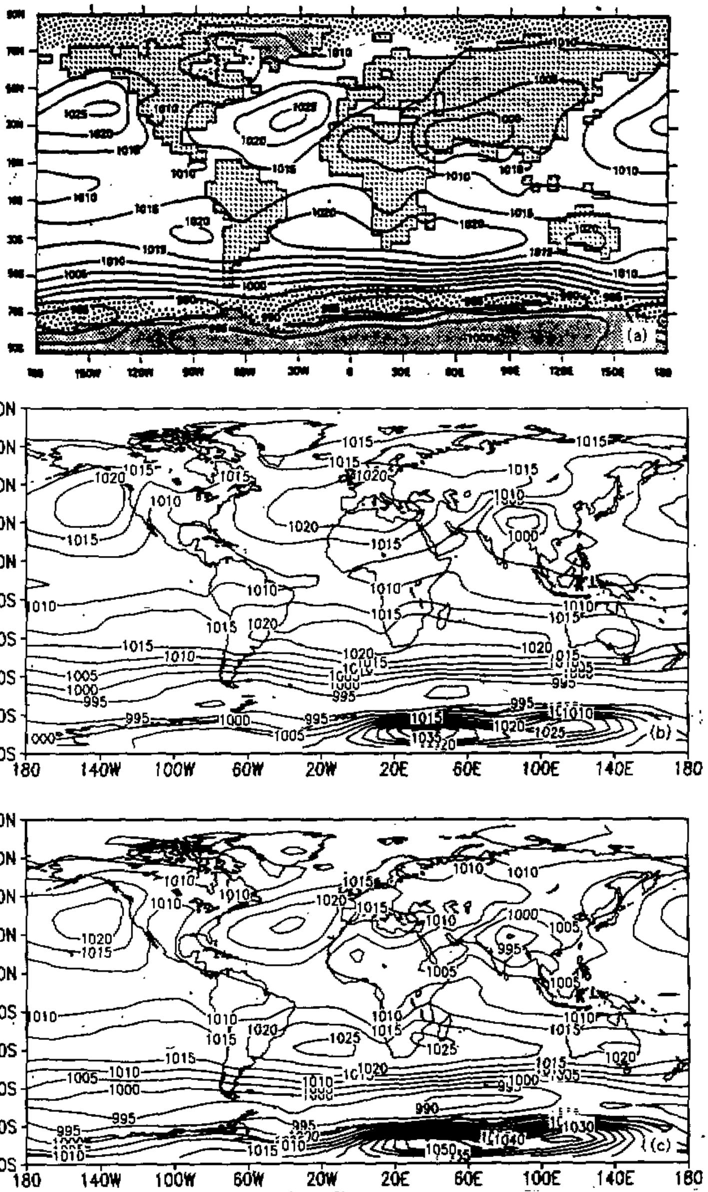

Fig. 6. Global distribution of sea surface pressure in July. (a): observation from Schlesinger and Gates(1980); (b): control AGCM run; (c): SSiB–AGCM run. Unit: hPa.

the tall trees are mainly located in tropical regions, Southeast Asia and the western Europe. The winter wheat is mainly located in East Asia, North America and the western Europe. The bare soil is mainly over central Asia and North Africa. As we will see in the following, these global differences will have strong impacts on the heat and water exchanges between the land

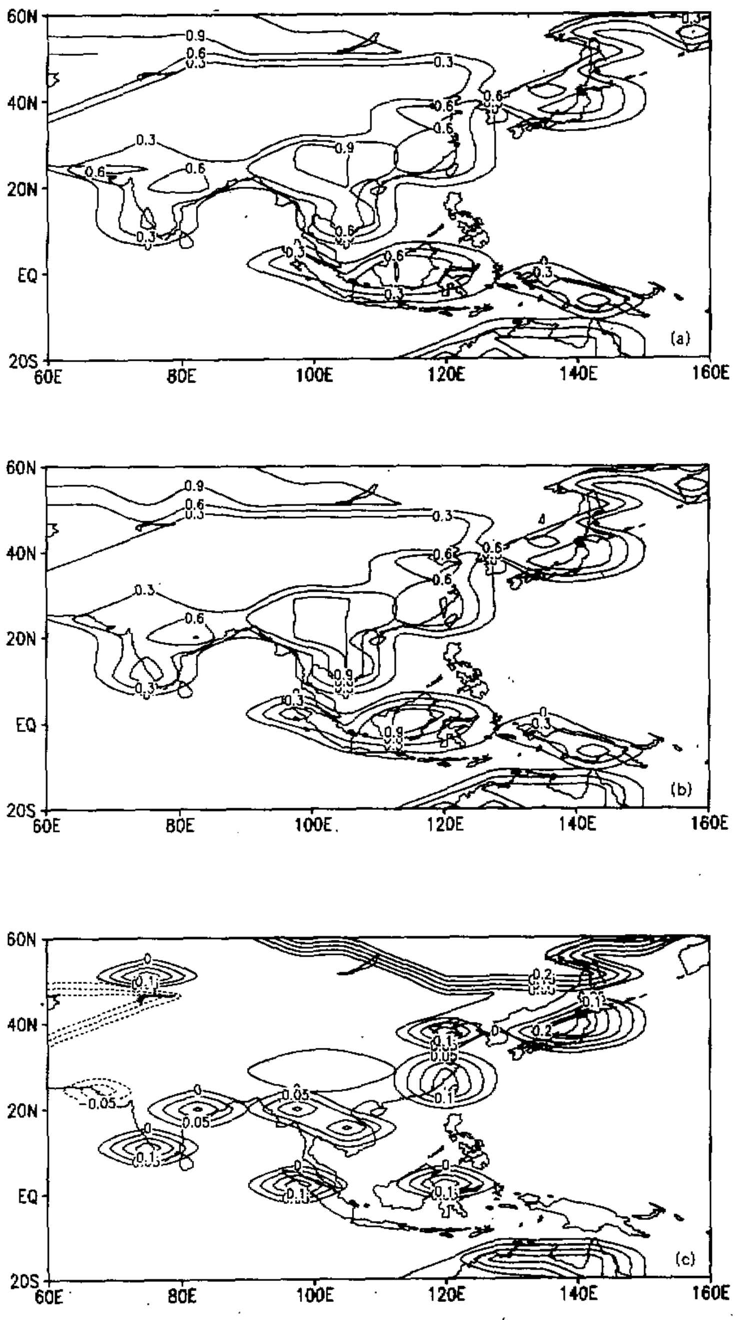
60N
40N
20N
EQ
20S
60E
80E
100E
120E
140E
160E
(a)
(b)
(c)

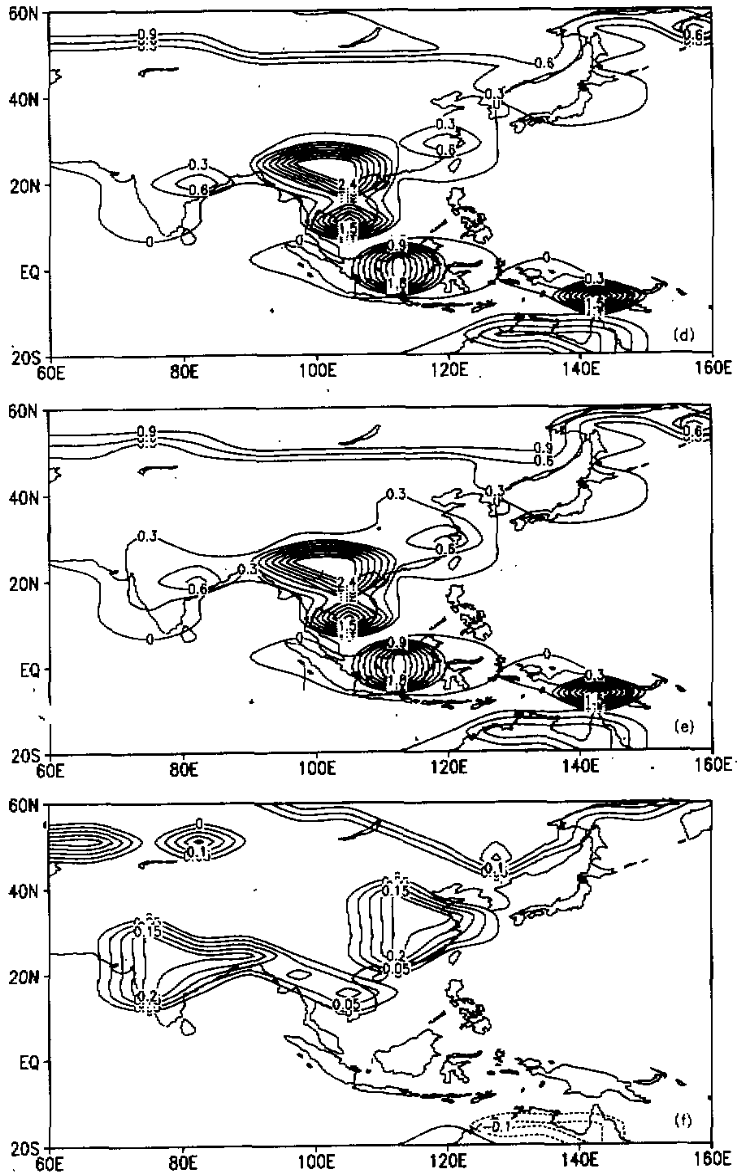

Fig. 7. The prescribed leaf greenness fraction (a–b) and roughness length (d–e) of April and June as well as their difference (June–April, c,f) in SSiB–AGCM. Roughness unit: m.

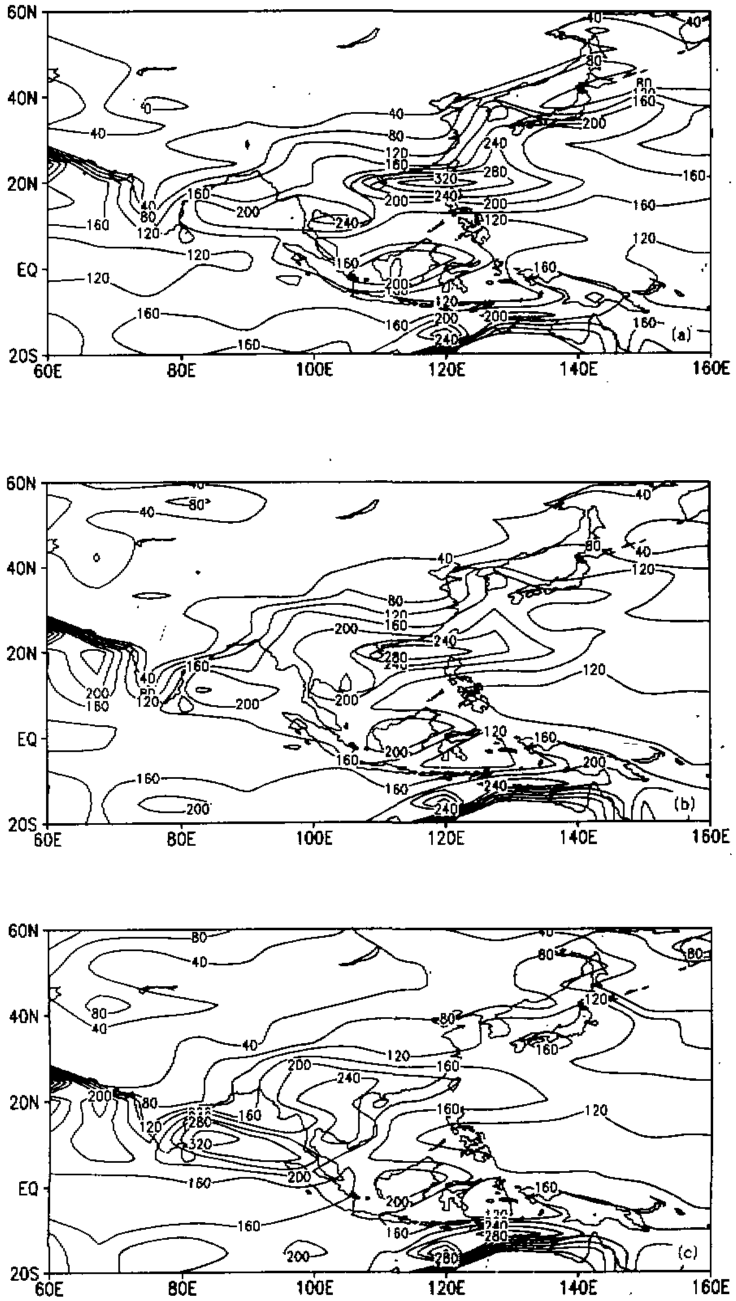
60N
40N
20N
EQ
20S
60E
80E
100E
120E
140E
160E
(a)
(b)
(c)

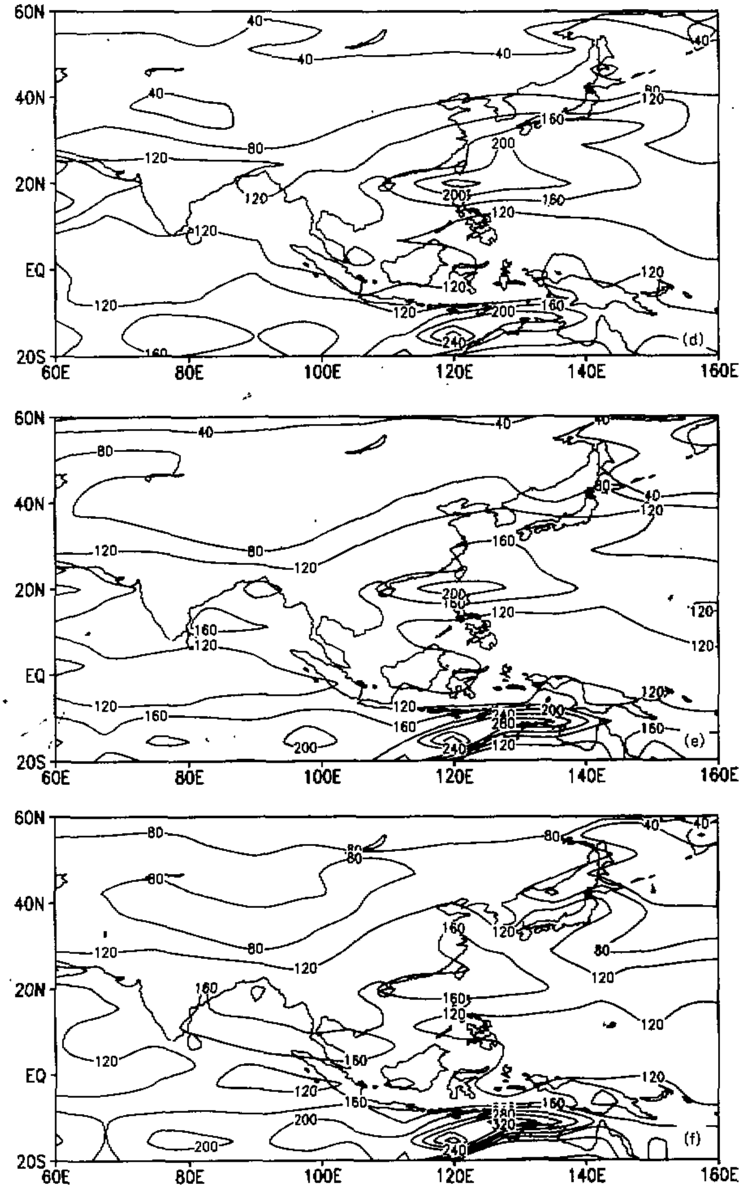

Fig. 8. Latent heat flux in April, May, and June, averaged for the last 15 years of the integrations. (a–c): SSiB–AGCM run; (d–f): control AGCM run. Unit: W / m^2.

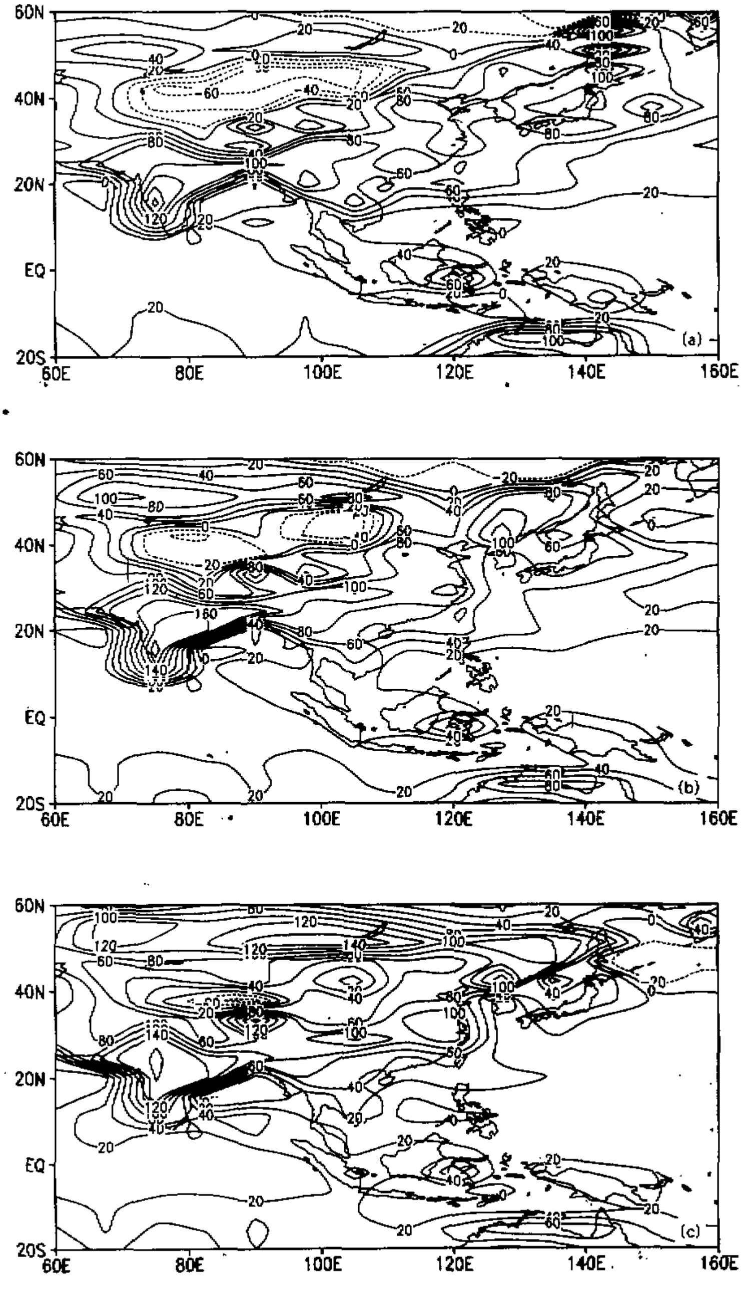
60N
40N
20N
EQ
20S
60E
80E
100E
120E
140E
160E
(a)
(b)
(c)

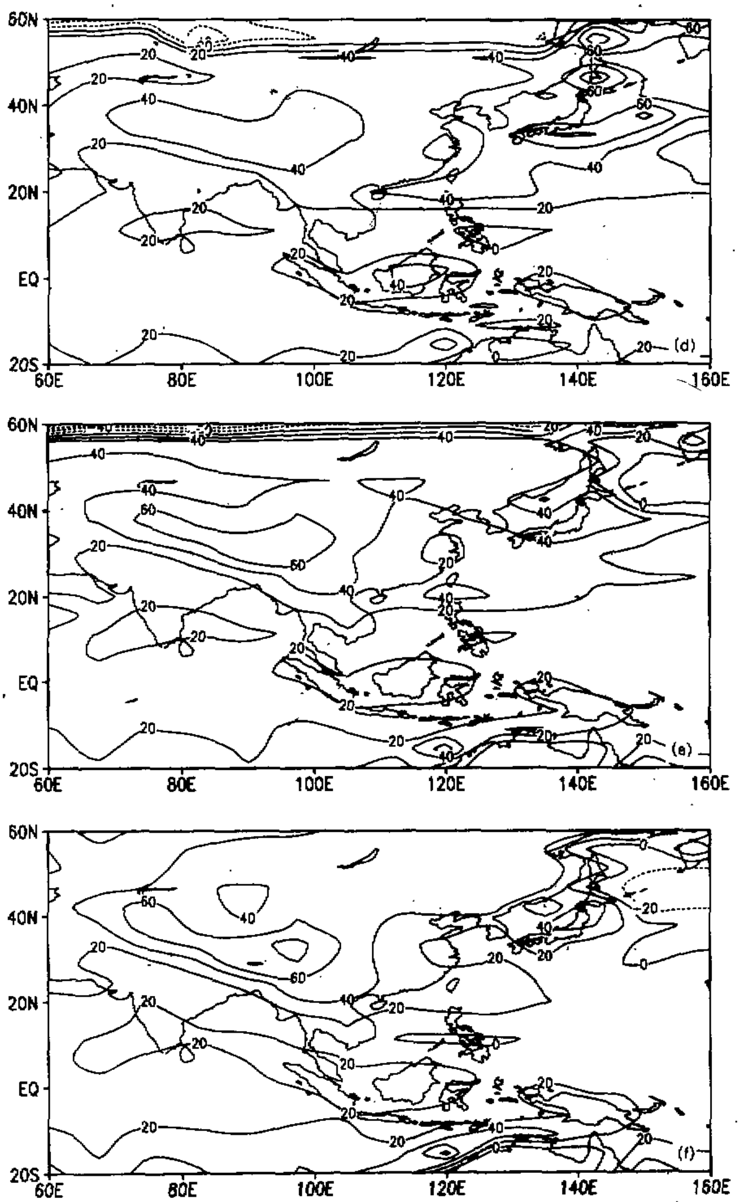

Fig. 9. Sensible heat flux in April, May, and June. (a–c): SSiB–AGCM run; (d–f): control AGCM run. Unit: W / m^2.

surface and the atmosphere.

The global distribution of the latent and sensible heat fluxes, averaged over the last fifteen years of the integrations, is presented in Fig. 3 for control AGCM and SSiB–AGCM respectively. The main feature of the latent heat flux is that it increases a lot over the tall trees areas, that is, the tropical forests and the forest over Northwest Europe. On the other hand, it decreases over the central Asia, North Africa and some parts of North America continent where are mainly covered bare soil with little ground vegetation. In these areas of bare soil, the sensible heat flux increases a lot to keep local heat balance. We note, however, that sensible heat increases also in some areas where the latent heat flux increases. We suspect that this may be due to the changes of the large scale atmospheric circulation and may not imply local heat imbalance.

These changes of the fluxes result in significant changes in precipitation or the diabatic heating. Fig. 4 presents the precipitation field for the two runs. The main characteristic is the

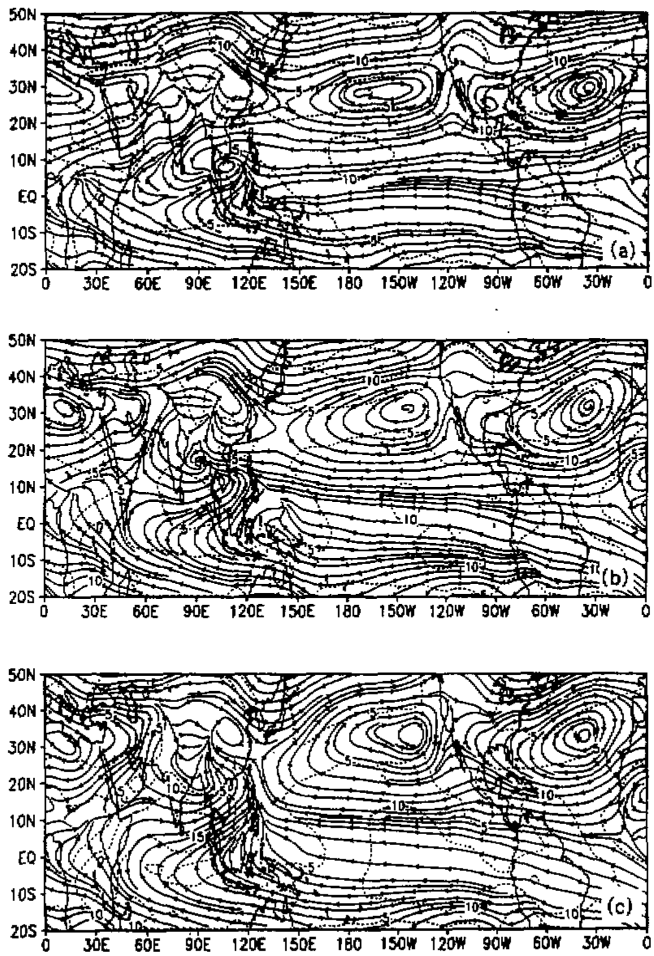

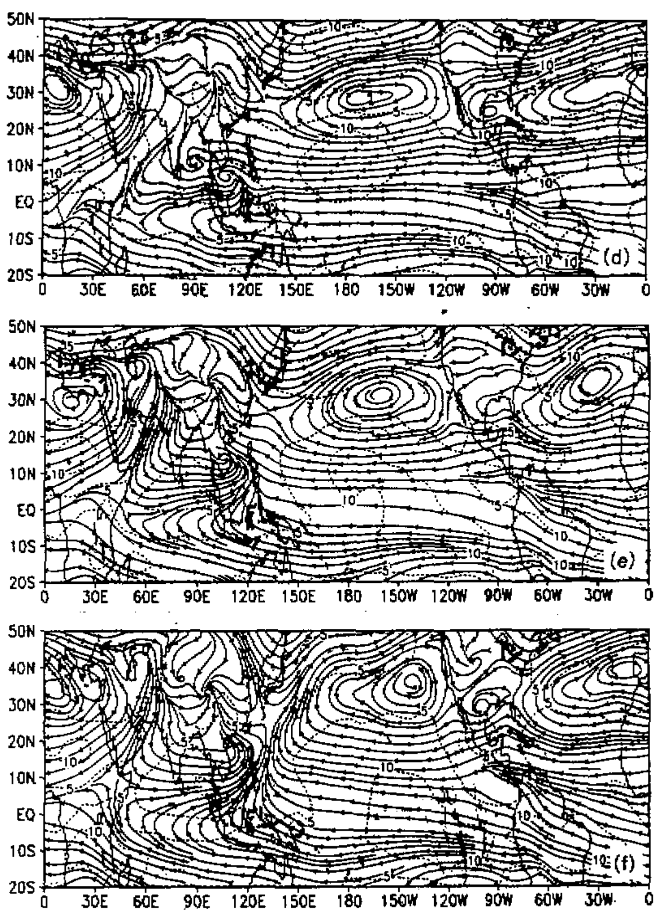

Fig. 10. 850 hPa streamline in April, May, and June. (a–c): SSiB–AGCM run; (d–f): control AGCM run. The dashed line is wind speed. Unit: m / s.

substantial reduction of precipitation over the areas of bare soil of the continents in the SSiB–AGCM run. For example, the precipitation over the central Asia and some parts of North America reduces to less than 2 mm / day. The observed three areas of more than 2 mm / day respectively over the western Europe, equatorial Africa, and Southeast Asia have been simulated reasonably well in the SSiB–AGCM run. In contrast, these areas are connected together in the control AGCM run. This makes the distribution of precipitation in the SSiB AGCM run much closer to observation (Fig. 4a). On the other hand, the precipitation over Southeast Asia increases a lot and the minimum of precipitation in the Yangtze River in control run almost disappears in SSiB run, which is also closer to observation. One exception is the precipitation over the equatorial Africa and it needs further study.

The improvement is also significant in surface temperature fields (Fig. 5). The temperature over most part of Asia, North America and Africa is generally a few degrees higher in SSiB run related to the increase of sensible heat flux. Obviously, it is much closer to the observation.

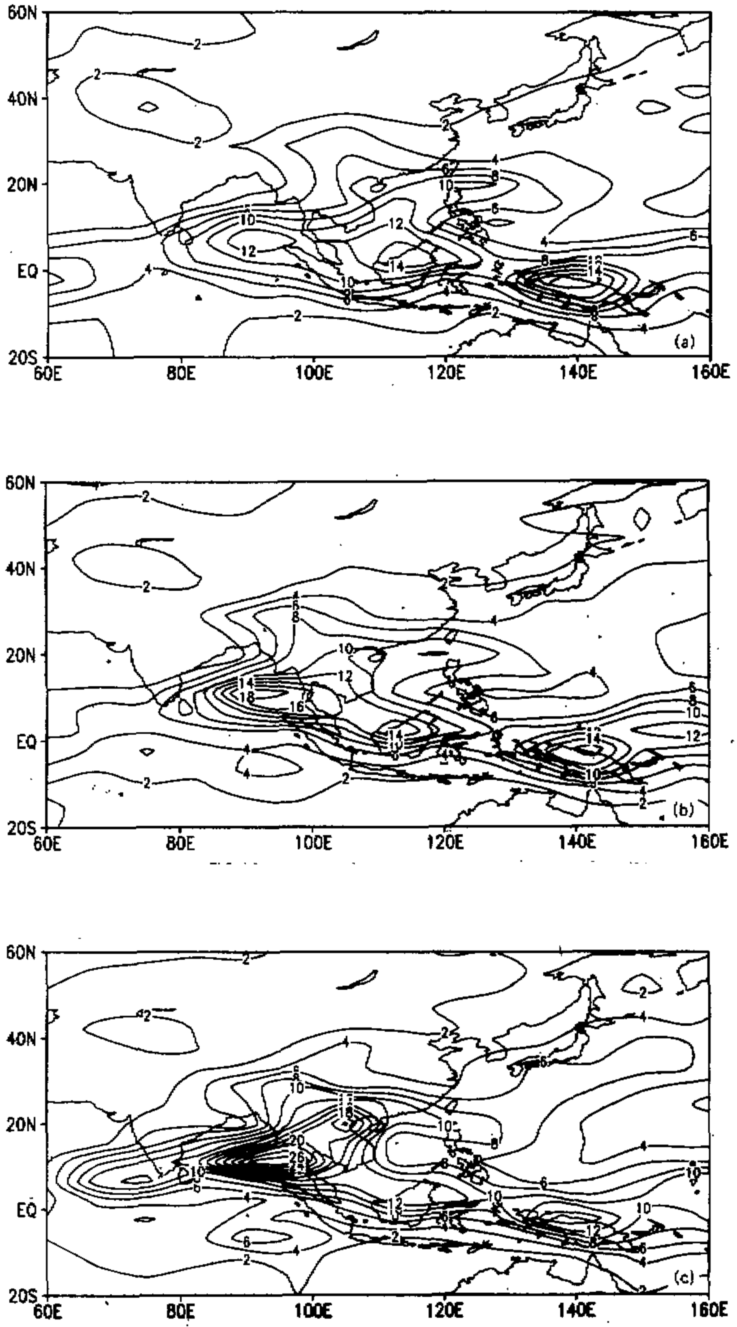
60N
40N
20N
EQ
20S
60E
80E
100E
120E
140E
160E
(a)
(b)
(c)

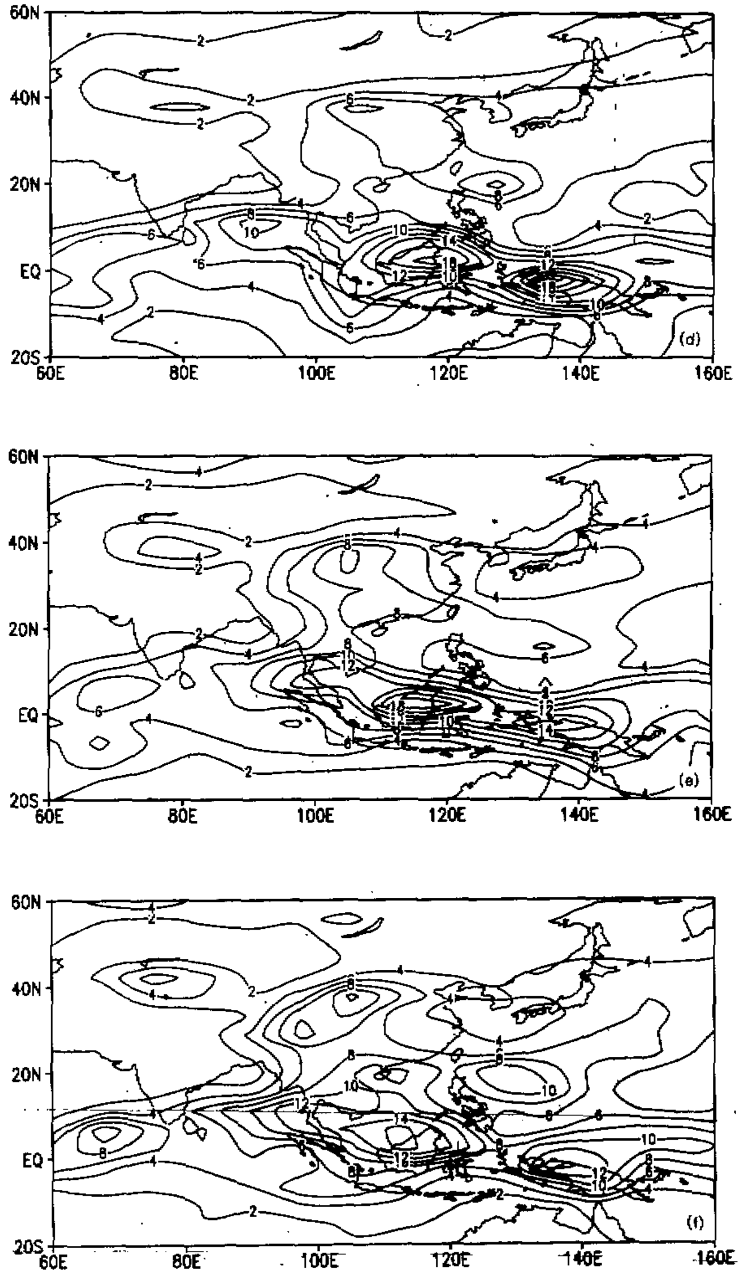

Fig. 11. Precipitation in April, May, and June. (a–c): SSiB–AGCM run; (d–f): control AGCM run. Unit: mm / day.

The improvement can also be detected from the comparison between the observed and simulated sea level pressure as shown in Fig. 6. Significant changes can be seen in the SSiB–AGCM results(Fig. 6c), in which the lows over Northeast Asia and North America become more prominent. These changes make the subtropical high isolines over North Atlantic closed and the low over Northeast Asia have better configuration of northeast–southwest tilting. The latter is thought to be very important indicator for precipitation over China. These improvements are related to the changes of surface temperature mentioned above.

The above demonstrates that the global differences in the characteristics of the land surface may have great impacts on the global distribution of climate of July.

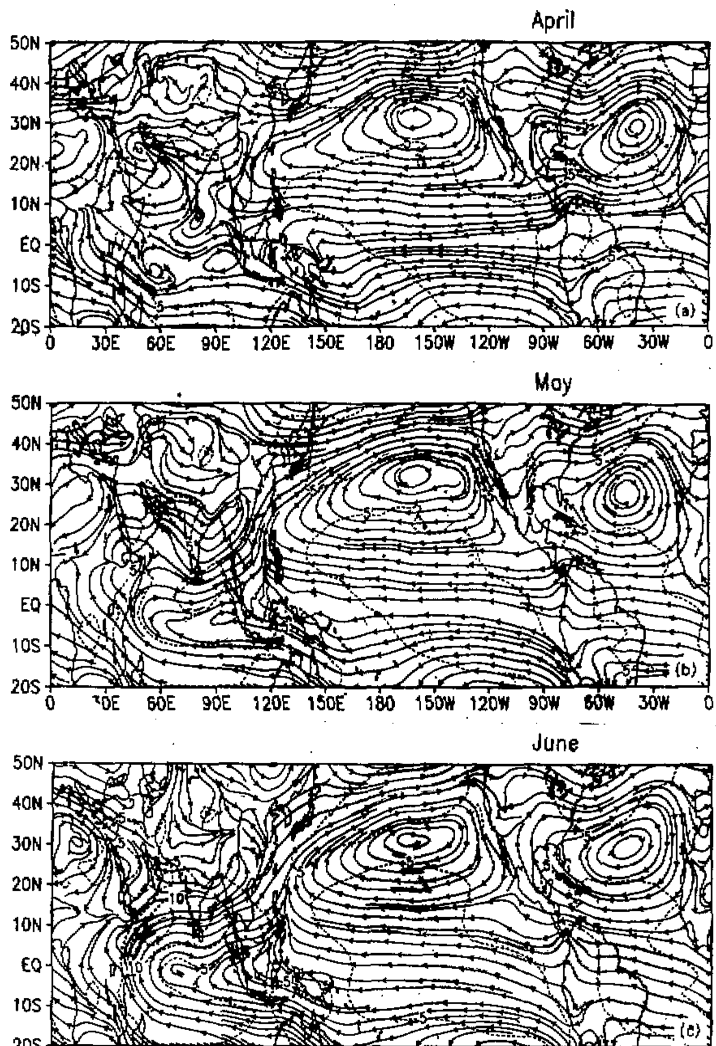

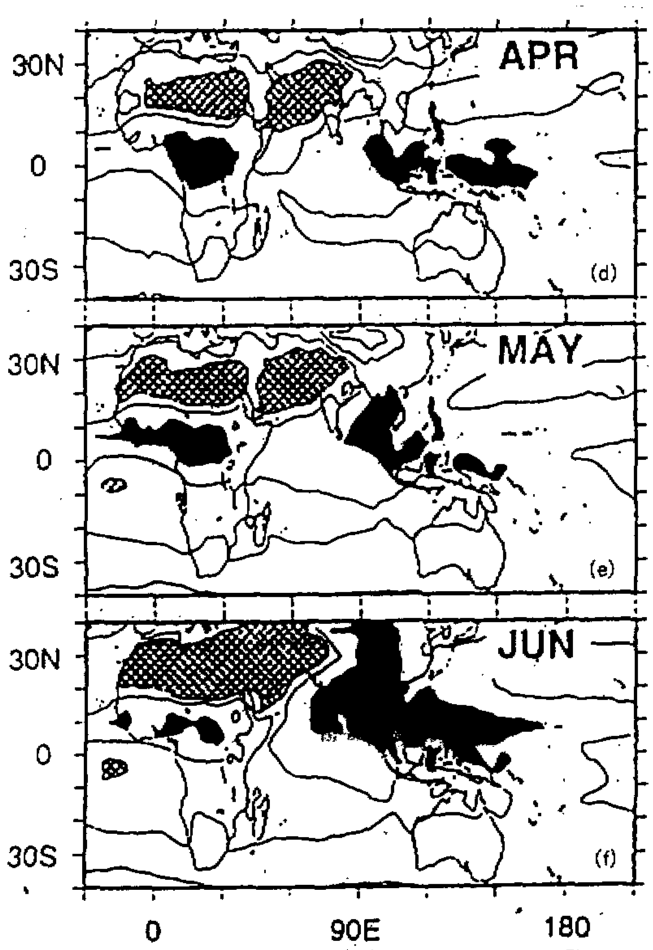

Fig. 12. (a–c): Observed 850 hPa streamline (from ECMWF analysis) and (d–f): OLR over East Asia (from Webster, 1995, shaded area is the minimum and stripped maximum) in April, May, and June. The dashed line in (a–c) is wind speed. Unit: m / s.

IV. ONSET OF SUMMER MONSOON

In SSiB, the prescribed characteristics of vegetation, such as roughness and leaf greenness, have significant seasonal variations. Fig. 7 shows the leaf greenness fraction and roughness for April and June over summer monsoon region. It can be seen clearly that from April to June the leaf greenness fraction increases evidently over mainland of China and India and the surface roughness increases about 0.1 m in these regions. These seasonal variations are the indications of the growing of vegetations there during that period.

The latent and sensible heat fluxes from April to June in SSiB–AGCM run have corresponding seasonal variation (Figs. 8a–c and 9a–c). It is clear that from April to June the latent heat flux over India and the Indo-China Peninsula increases remarkably and the maximum centres move northwestward evidently. The sensible heat flux also increases over India and the Tibetan plateau and has northwestward extension. In control AGCM run, however, there are no such evident northwestward extensions (Figs. 8d-f and 9d-f). These differences will definitely have impacts on the onset of summer monsoon.

The 850 hPa wind from April to June simulated in the SSiB-AGCM run is shown in Figs. 10(a-c). It can be seen that the establishment of the cross-equatorial Somali jet and the South China Sea jet in May is well simulated. In June, the two jets become stronger and the associated southwesterly wind reaches the South China Sea. In the control AGCM run (Figs. 10d-f), however, the Somali jet does not appear in May and is only established in June. In addition, in the control AGCM run, the southwesterly does not reach the South China Sea and Japan. Obviously, the simulation of SSiB-AGCM is much closer to observation (Figs. 12a-c).

Similar situation occurs in precipitation field. In the SSiB-AGCM run , prominent northwestward march of precipitation can be identified over India and China (Figs. 11a-c), which is close to observation (Figs. 12d-f). In the control AGCM run, however, the precipitation does not extend northwestward enough to the observed latitudes during the period of April to June (Figs. 11d-f).

VI. SUMMARY

A simple biosphere model (SSiB) is implemented into the LASG / IAP spectral AGCM and it is shown that the implement of the land surface processes greatly improves the model's simulation of July mean climate and seasonal variations, such as onset of summer monsoon. It proves that the global differences in characteristics of the land surface are important for global distribution of the July climate and the seasonal variations of the land surface characteristics are very important for the seasonal variation of climate, such as the onset of summer monsoon.

The authors would like to thank Dr. Xue Yongkong for his kind helps in providing the SSiB model for the AGCM and Prof. Sun Shufeng for his helpful discussions with the authors.

REFERENCES

Dorman, J.L. and P. Sellers (1989), A global climatology of albedo, roughness length and stomatal resistance for atmospheric general circulation models as represented by the SiB, *J. Appl. Meteor.*, **28**: 833-855.

Klink, K, and C.J. Willmott (1985), *Notes on a global vegetation data set for use in GCMs*, Univ. of Delaware, Newark, Delaware 175 pp.

Kuchler, A.W. (1983), *World map of natural vegetation*, Goode's World Atlas, 16th edition, Rand McNally, 16-17.

Sato, N.P., P.J. Sellers, D.A. Randal, E.K. Schneider, J. Shukla, J.L. Kinter III, Y-T. Hou and E. Albertazzi (1989), Effects of implementing the simple biosphere model in a general circulation model, *J. Atmos. Sci.*, **46**: 2757-2782.

Sellers, P.J., Y. Mintz, Y.C. Sud, and A. Dalcher (1986), A simple biosphere model(SiB) for use within general circulation models, *J. Atmos. Sci.*, **43**: 505-531.

Wu G-X., H. Liu, Y-C. Zhao, and W-P. Li (1996), A nine-layer atmospheric general circulation model and its performance, *Adv. in Atmos. Sci.*, **13**: 1-18.

Xue Y., P.J. Sellers, J.L. Kinter and J. Shukla (1991), A simplified biosphere model for global climate studies, *J. Climate*, **4**: 345-364.